Bulletin of the JSME Vol.9, No.1, 2014
Journal of Biomechanical Science and Engineering

Numerical analysis of arterial contraction regulated by smooth muscle stretch and intracellular calcium ion concentration

Naoki KIDA* and Taiji ADACHI*
* Department of Biomechanics, Institute for Frontier Medical Sciences, Kyoto University
53 Kawahara-cho, Shogoin, Sakyo, Kyoto 606-8507, Japan
E-mail: adachi@frontier.kyoto-u.ac.jp

Received 23 October 2013

Abstract
In this study, for a better understanding of arterial functions, we examine the effects of active stresses, which are generated by contractile units included in smooth muscle cells, on the stress distribution in the arterial wall. Thus far, it is widely recognized that active stress generation is regulated by mechanical and chemical operations, i.e., both smooth muscle stretch and intracellular calcium ion concentration. Based on this fact, we develop an arterial wall model with active stresses that couples the mechanical and chemical ones suitable for the finite element method. By using this coupled model within the framework of finite element analysis, we calculate the stress distribution including active stresses at a prescribed intracellular calcium ion concentration. The results show that as the intracellular calcium ion concentration increases, the effect of active stress appears continuously, i.e., stress distribution could be considered as a continuous function of the intracellular calcium ion concentration. To obtain stress distributions at the prescribed intracellular calcium ion concentration, which is assumed to be reached as a result of active calcium ion transport under various in vivo conditions, are meaningful as a preliminary step in developing advanced models considering the active calcium ion transport systems.

Key words : Artery, Active stress, Mechanochemical model, Intracellular calcium ion concentration, Smooth muscle stretch, Nonlinear finite element method

1. Introduction

Arteries consist of an inner, middle, and outer layer (Gasser et al., 2006). Of these, the middle layer is the most important, because it contains smooth muscle cells that generate active stresses and allow an arterial wall to constrict or dilate. This activity buffers the circumferential wall stresses caused by external loads, controls the lumen diameter, and regulates local blood flow (Humphrey and Na, 2002). Active stress generation is an important physiological phenomenon that must be considered from a mechanical viewpoint. Therefore, it is important to develop a solid-mechanics-based arterial model and to analyze it through numerical simulations. In the field of clinical medicine, such a mechanical model and analysis could be used to evaluate physiological functions, predict pathogenesis, and improve treatment of diseases, e.g., atherosclerosis and aneurysms. For example, the three-dimensional contour plots of stress distribution obtained via mechanical analysis for each patient will provide useful information about where pathological changes occur.

Thus far, many mechanical models of active stresses have been proposed and analyzed numerically (Rachev and Hayashi, 1999; Zulliger et al., 2004; Stålhand et al., 2008, 2011; Murtada et al., 2010a,b; Schmitz and Böl, 2011; Böl et al., 2012). When modeling active stresses from a mechanical standpoint, the phenomenological strain-energy function as a function of smooth muscle stretch is widely used. At a microlevel, active stresses are generated by contractile units that are included in the smooth muscle cells. It is believed that relative slidings between actin and myosin filaments in a contractile unit generate active stresses. In this sliding model, a contractile unit transitions through four chemical states owing to the chemical reaction regulated by the intracellular calcium ion concentration. The intracellular calcium ions are the primary determinant of the contractility; increases in intracellular calcium concentration lead to contraction (600-800 nM in fully contracted smooth muscle) while decreases lead to relaxation (100 nM in resting smooth muscle) (Murtada et al., 2010a). A contractile unit generates active stresses, only when it reaches certain chemical states (Hai and Murphy,

Paper No.13-00262
[DOI: 10.1299/jbse.2014jbse0002]

1988). As described above, active stress generation is controlled by both smooth muscle stretch and intracellular calcium ion concentration. Therefore, it is necessary to analyze active stresses by coupling a mechanical model with a chemical one. Thus far, these two models have been studied individually, but few studies have focused on investigations using a mechanochemical model.

In this study our primary objective is to develop an arterial wall model with active stresses that couples the mechanical one proposed by Schmitz and Böl (2011) and chemical one proposed by Hai and Murphy (1988) suitable for the finite element method. By using this coupled model within the framework of finite element analysis, we calculate the stress distribution including active stresses generated by vascular smooth muscle cells at a prescribed intracellular calcium ion concentration. Knowing the stress distribution at each prescribed intracellular calcium ion concentration can be helpful for understanding active calcium ion transport systems, because alterations in the stress distribution caused by the variation of external loads are buffered by proper active stress generation resulting from continuous intracellular calcium ion concentration changes through active calcium ion transport systems.

2. Vascular mechanics basis for finite element analysis

Because arteries show geometrical and material nonlinearities, a numerical approach using nonlinear finite element methods is used. Furthermore, arteries are modeled by an incompressible hyperelastic material (Fung et al., 1979; Weiss et al., 1996). In this section, we describe the notations used in this paper and the variational principle that we select to discretize the problem.

2.1. Separation of deformation gradient tensor and strain-energy function

The particle positions in the reference configuration Ω_0 and the current configuration Ω are denoted as $\boldsymbol{X}$ and $\boldsymbol{x}$, respectively. We assume that a bijection φ exists such that $\boldsymbol{x} = \varphi(\boldsymbol{X})$. The deformation gradient $\boldsymbol{F}$ with Jacobian $J = \det \boldsymbol{F} > 0$ is then defined as $\boldsymbol{F} = \partial\varphi(\boldsymbol{X})/\partial\boldsymbol{X}$, and the right Cauchy-Green tensor is defined as $\boldsymbol{C} = \boldsymbol{F}^{\mathrm{T}}\boldsymbol{F}$. In finite element methods, the material description is treated separately as volumetric and isochoric parts. The deformation gradient tensor $\boldsymbol{F}$ is split into two components as

$$\boldsymbol{F} = J^{1/3}\,\bar{\boldsymbol{F}}, \tag{1}$$

where the overbar $\bar{(\cdot)}$ denotes the isochoric contributions of certain physical quantities. The $J^{1/3}\boldsymbol{I}$ term is associated with volumetric deformations, whereas $\bar{\boldsymbol{F}}$ is associated with isochoric deformations of the material (Holzapfel, 2000).

We consider a slightly compressible two-fiber reinforced anisotropic hyperelastic material that postulates the existence of a strain-energy function Ψ (defined per unit reference volume). The second Piola-Kirchhoff stress tensor $\boldsymbol{S}$ is expressed as $\boldsymbol{S} = 2\partial\Psi/\partial\boldsymbol{C}$. The strain-energy function Ψ is assumed to be uncoupled, in which the volumetric and isochoric components are such that

$$\Psi = \Psi_{\mathrm{vol}}(J) + \Psi_{\mathrm{iso}}(\bar{I}_1, \bar{I}_2, \cdots, \bar{I}_9), \tag{2}$$

where $\bar{I}_1, \cdots, \bar{I}_9$ are the isochoric contributions of invariants of $\boldsymbol{C}$ and structural tensors. The purely volumetric part

$$\Psi_{\mathrm{vol}}(J) = \frac{\kappa}{2}(J-1)^2 \tag{3}$$

controls the degree of incompressibility by means of the positive parameter κ (Brink and Stein, 1996). In the following sections, the isochoric contributions of the passive and active strain-energy functions of an arterial wall are given.

2.2. Variational principle of saddle type

The constrained-elastostatic boundary-value problem, such as a slightly compressible material response (i.e., $J \simeq 1$), is equivalent to finding the saddle point $(\boldsymbol{u}, p)$ of the functional $\Pi_{\mathrm{PL}}(\boldsymbol{u}, p)$ (Brink and Stein, 1996; Chang et al., 1991; Sussman and Bathe, 1987). The two-field functional is expressed as

$$\Pi_{\mathrm{PL}}(\boldsymbol{u}, p) = \int_{\Omega_0}\left[p\{J(\boldsymbol{u}) - 1\} - \frac{p^2}{2\kappa} + \Psi_{\mathrm{iso}}(\bar{I}_1, \bar{I}_2, \cdots, \bar{I}_9)\right]dV + \Pi_{\mathrm{ext}}(\boldsymbol{u}), \tag{4}$$

where $\boldsymbol{u}$ is the displacement vector; p, an additional Lagrangian multiplier; and the functional $\Pi_{\mathrm{ext}}(\boldsymbol{u})$, the potential of conservative exterior forces.

Weak-form equations derived from the functional $\Pi_{\mathrm{PL}}(\boldsymbol{u}, p)$ are generally nonlinear in unknown fields $\boldsymbol{u}$ and p. To implement weak-form equations in mixed finite element methods, they must be linearized and solved by an iterative

[DOI: 10.1299/jbse.2014jbse0002]

method, e.g., the Newton-Raphson method. The derivation of weak-form equations and the linearization procedure are detailed in Brink and Stein (1996); Rüter and Stein (2000).

3. Modeling an arterial wall with active stresses

This section describes the passive mechanical and active mechanochemical model of the arterial wall. For the active stresses, we couple the chemical and the mechanical model.

3.1. Strain energy function for the passive response

We adopt the passive mechanical model proposed by Holzapfel et al. (2000, 2004). In this model, the arterial wall is composed of an isotropic material, and two families of collagen fibers, which characterize the anisotropy, are helically wound along the arterial axis, as indicated in **Fig.** 1. The fiber contribution is modeled using a pair of preferred directional unit vectors $\boldsymbol{a}_0$ and $\boldsymbol{g}_0$. In the local covariant basis of the cylindrical coordinate system $\{\boldsymbol{e}_R, \boldsymbol{e}_\Theta, \boldsymbol{e}_Z\}$, $\boldsymbol{a}_0$ and $\boldsymbol{g}_0$ take the following forms:

$$\boldsymbol{a}_0 = 0\,\boldsymbol{e}_R + \cos\eta\,\boldsymbol{e}_\Theta + \sin\eta\,\boldsymbol{e}_Z, \tag{5a}$$

$$\boldsymbol{g}_0 = 0\,\boldsymbol{e}_R + \cos\eta\,\boldsymbol{e}_\Theta - \sin\eta\,\boldsymbol{e}_Z, \tag{5b}$$

where η is the angle between fibers and the circumferential direction, as indicated in **Fig.** 1. The isochoric term of this (passive) strain-energy function depends on the three invariants $\bar{I}_1$, $\bar{I}_4$, and $\bar{I}_6$, and it is given by

$$\Psi_{\text{pas,iso}}(\bar{\boldsymbol{C}}, \boldsymbol{a}_0 \otimes \boldsymbol{a}_0, \boldsymbol{g}_0 \otimes \boldsymbol{g}_0) = c_e(\bar{I}_1 - 3) + \frac{c_1}{2c_2}\sum_{i=4,6}\left[\exp\{c_2(\bar{I}_i - 1)^2\} - 1\right], \tag{6}$$

where $c_e > 0$, $c_1 > 0$, and $c_2 > 0$ are material parameters. The first term on the right-hand side of this equation is an isotropic contribution that depends on an invariant $\bar{I}_1$, expressed as $\mathrm{tr}\bar{\boldsymbol{C}}$. The second anisotropic term on the right-hand side of this equation contributes only when the fibers are extended, i.e., when $\bar{I}_4 > 1$ or $\bar{I}_6 > 1$, where $\bar{I}_4 = \boldsymbol{a}_0 \cdot \bar{\boldsymbol{C}}\boldsymbol{a}_0$ and $\bar{I}_6 = \boldsymbol{g}_0 \cdot \bar{\boldsymbol{C}}\boldsymbol{g}_0$.

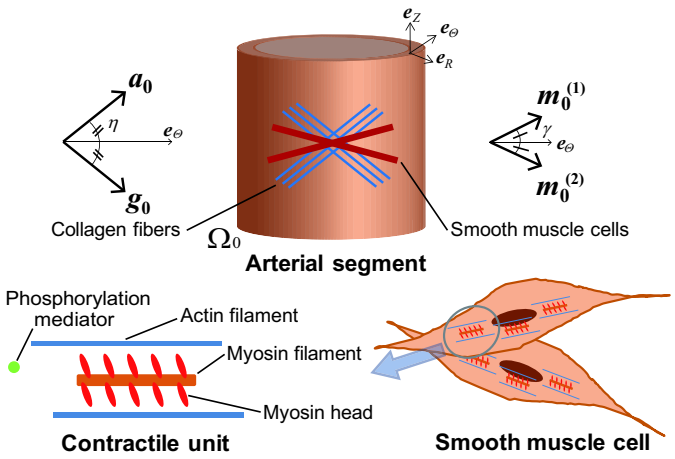

Fig. 1 Schematic of arterial components: An artery comprises a noncollagenous matrix, two families of fibers, and two families of smooth muscle cells. The reference directions of the two families of fibers and two families of smooth muscle cells are represented by the unit vectors $\boldsymbol{a}_0$ and $\boldsymbol{g}_0$ and the unit vectors $\boldsymbol{m}_0^{(1)}$ and $\boldsymbol{m}_0^{(2)}$, respectively. A smooth muscle cell contains many contractile units. A basic contractile unit comprises two actin filaments and one myosin filament connected by many myosin heads. The set $\{\boldsymbol{e}_R, \boldsymbol{e}_\Theta, \boldsymbol{e}_Z\}$ is the local covariant basis of the cylindrical coordinate system.

3.2. Chemical model for active stresses

Active stresses are generated by contractile units included in smooth muscle cells as shown in **Fig.** 1. Contractile units, which are essentially one-dimensional structures, are aligned along the axis of smooth muscle cells, and they comprise actin filaments, myosin filaments, and myosin heads. Actin and myosin filaments can slide against each other

[DOI: 10.1299/jbse.2014jbse0002]

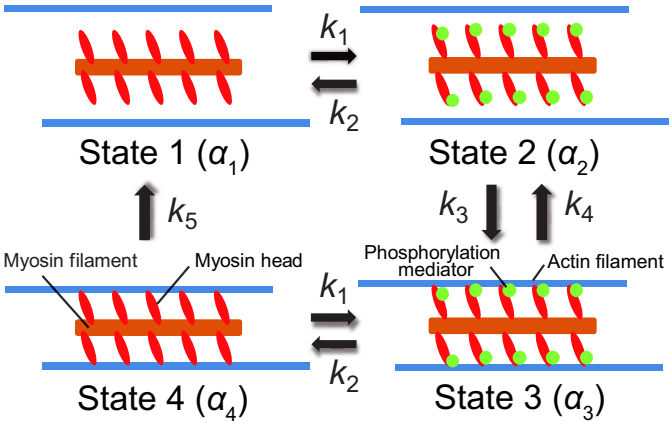

Fig. 2 Schematic of chemical model proposed by Hai and Murphy (1988): α_1, α_2, α_3, and α_4 represent the chemical state fractions of the myosin head and $k_1, \cdots, k_5$ are reaction rates. The phosphorylation of the myosin head is controlled by calcium ions.

by means of chemically driven forces from the myosin heads, as indicated in **Fig.** 2. These relative slidings generate active stresses and are regulated by the intracellular calcium ion concentration.

To determine the active stress generating states of the contractile units, we use the model proposed by Hai and Murphy (1988). This model describes the following four chemical states of contractile units: a free unphosphorylated myosin head (State 1), phosphorylated myosin head (State 2), phosphorylated myosin head attached to actin (State 3), and dephosphorylated myosin head attached to actin (State 4). The last two states are active stress generating states. This actin-myosin sliding model is described as a coupled system of first-order ordinary differential equations in time $t \in [0, \infty)$ for four chemical state fractions $\boldsymbol{\alpha} = (\alpha_1, \alpha_2, \alpha_3, \alpha_4)^{\mathrm{T}}$ as

$$\begin{bmatrix} \dot{\alpha}_1 \\ \dot{\alpha}_2 \\ \dot{\alpha}_3 \\ \dot{\alpha}_4 \end{bmatrix} = \begin{bmatrix} -k_1 & k_2 & 0 & k_5 \\ k_1 & -(k_2+k_3) & k_4 & 0 \\ 0 & k_3 & -(k_4+k_2) & k_1 \\ 0 & 0 & k_2 & -(k_1+k_5) \end{bmatrix} \begin{bmatrix} \alpha_1 \\ \alpha_2 \\ \alpha_3 \\ \alpha_4 \end{bmatrix}. \tag{7}$$

In matrix notation, this model is expressed as $\dot{\boldsymbol{\alpha}} = \boldsymbol{K}\boldsymbol{\alpha}$, where $k_1, \cdots, k_5$ are chemical rate constants. Because α_i ($i = 1, 2, 3, 4$) are fractions, they satisfy the constraint $\sum_{i=1}^{4} \alpha_i = 1$. Typical initial conditions are $\alpha_1 = 1$ and $\alpha_2 = \alpha_3 = \alpha_4 = 0$, specifying fully relaxed tissues. In this chemical model, it is assumed that the intracellular calcium ion concentration regulates a single parameter, namely, the reaction rate k_1 of myosin head phosphorylation.

At a chemically steady state ($t \to \infty$), Eq. (7) with constraints is expressed as

$$\begin{bmatrix} 0 \\ 0 \\ 0 \\ 0 \\ 1 \end{bmatrix} = \begin{bmatrix} -k_1 & k_2 & 0 & k_5 \\ k_1 & -(k_2+k_3) & k_4 & 0 \\ 0 & k_3 & -(k_4+k_2) & k_1 \\ 0 & 0 & k_2 & -(k_1+k_5) \\ 1 & 1 & 1 & 1 \end{bmatrix} \begin{bmatrix} \alpha_1 \\ \alpha_2 \\ \alpha_3 \\ \alpha_4 \end{bmatrix} \tag{8}$$

or $\boldsymbol{b} = \boldsymbol{K}_{\mathrm{c}}\boldsymbol{\alpha}$ in matrix notation. The solutions of this overdetermined linear system are replaced by finding the minimization point $\boldsymbol{\alpha}$ of the Euclidean norm $\| \boldsymbol{b} - \boldsymbol{K}_{\mathrm{c}}\boldsymbol{\alpha} \|$.

3.3. Strain energy function for active stress

Smooth muscle cells are helically aligned along the arterial axis and are modeled using a pair of preferred directional unit vectors $\boldsymbol{m}_0^{(1)}$ and $\boldsymbol{m}_0^{(2)}$ at point $\boldsymbol{X} \in \Omega_0$, as indicated in **Fig.** 1. Similar to Eqs. (5a) and (5b), the directional vectors

[DOI: 10.1299/jbse.2014jbse0002]

$\boldsymbol{m}_0^{(1)}$ and $\boldsymbol{m}_0^{(2)}$ take the following forms:

$$\boldsymbol{m}_0^{(1)} = 0\,\boldsymbol{e}_R + \cos\gamma\,\boldsymbol{e}_\Theta + \sin\gamma\,\boldsymbol{e}_Z, \tag{9a}$$

$$\boldsymbol{m}_0^{(2)} = 0\,\boldsymbol{e}_R + \cos\gamma\,\boldsymbol{e}_\Theta - \sin\gamma\,\boldsymbol{e}_Z, \tag{9b}$$

where γ is the angle between the smooth muscle cells and the circumferential direction. Deformed smooth muscle cells at the associated points $\boldsymbol{x} \in \Omega$ are defined by a pair of directional unit vectors $\boldsymbol{m}^{(1)}$ and $\boldsymbol{m}^{(2)}$. The relationship between $\boldsymbol{m}_0^{(i)}$ and $\boldsymbol{m}^{(i)}$ is expressed as $\overline{\boldsymbol{F}}\boldsymbol{m}_0^{(i)} = \overline{\lambda}_{\mathrm{m}}^{(i)}\boldsymbol{m}^{(i)}$, where $\overline{\lambda}_{\mathrm{m}}^{(i)}$ is the isochoric stretch of smooth muscle cells $\boldsymbol{m}_0^{(i)}$ $(i = 1, 2)$.

To incorporate active stresses into a constitutive model, we use the approach of Schmitz and Böl (2011). This phenomenological model is based on the concept of embedded fibers that expand or contract self-actively in the direction of $\boldsymbol{m}_0^{(i)}$ $(i = 1, 2)$. The isochoric contribution of the active strain-energy function $\Psi_{\mathrm{act,iso}}$, which depends on $\overline{\lambda}_{\mathrm{m}}^{(i)}$ and chemical state fractions α_3 and α_4, is modeled as a polynomial of $\overline{\lambda}_{\mathrm{m}}^{(i)}$ and is given by

$$\Psi_{\mathrm{act,iso}}(\overline{\lambda}_{\mathrm{m}}^{(i)},\ \alpha_3,\ \alpha_4) = (\alpha_3 + \alpha_4)\sum_{n=0}^{5} a_n(\overline{\lambda}_{\mathrm{m}}^{(i)})^n, \tag{10}$$

where a_n $(n = 0, \cdots, 5)$ are material parameters. The original Schmitz model does not explicitly take into account the effect of the intracellular calcium ion concentration. In their model, the chemical state fraction $\alpha_3 + \alpha_4$ is treated as a constant. In this study, we consider that the fractions $\alpha_1, \cdots, \alpha_4$ vary with intracellular calcium ion concentration as described in the next subsection.

3.4. Relation between the reaction rate k_1 and intracellular calcium ion concentration

At a chemically steady state $(\dot{\alpha}_i \to 0,\ t \to \infty,\ i = 1, 2, 3, 4)$, from Eq. (7), the rate constant k_1 is given as a function of the fraction of phosphorylated myosin heads $\alpha_2 + \alpha_3$, i.e.,

$$k_1 = k_2\frac{\alpha_2 + \alpha_3}{\alpha_1 + \alpha_4} = k_2\frac{\alpha_2 + \alpha_3}{1 - (\alpha_2 + \alpha_3)}. \tag{11}$$

The relationship between the intracellular calcium ion concentration $\beta(\boldsymbol{x})$ in the current configuration Ω and fraction of phosphorylated myosin heads $\alpha_2 + \alpha_3$ is fitted into a sigmoidal function commonly encountered in enzyme reaction approximations, i.e.,

$$\alpha_2 + \alpha_3 = a + \frac{b}{1 + 10^{-c\beta(\boldsymbol{x})+d}}, \tag{12}$$

where a, b, c, and d are constants (Murtada et al., 2010b).

From Eqs. (11) and (12), the rate constant k_1 is defined as a function of the intracellular calcium ion concentration $\beta(\boldsymbol{x})$. Substituting the rate k_1 into Eq. (8), the fractions $\alpha_1, \cdots, \alpha_4$ as functions of $\beta(\boldsymbol{x})$ are obtained.

3.5. Sum of strain-energy function

From Eqs. (2), (3), (6), and (10), the material behavior is described by means of the total strain-energy function as

$$\Psi = \Psi_{\mathrm{vol}}(J) + \Psi_{\mathrm{pas,iso}}(\overline{\boldsymbol{C}},\ \boldsymbol{a}_0 \otimes \boldsymbol{a}_0,\ \boldsymbol{g}_0 \otimes \boldsymbol{g}_0) + \sum_{i=1,2}\frac{1}{2}\Psi_{\mathrm{act,iso}}(\overline{\lambda}_{\mathrm{m}}^{(i)},\ \beta(\boldsymbol{x})), \tag{13}$$

where $1/2$ is the weighting function with respect to the muscle cell $\boldsymbol{m}_0^{(i)}$. In finite element methods described by the total Lagrangian formulation, the second Piola-Kirchhoff stress tensor $\boldsymbol{S} = 2\partial\Psi/\partial\boldsymbol{C}$ and fourth-order elasticity tensor $\mathbb{C} = 2\partial\boldsymbol{S}/\partial\boldsymbol{C}$ must be calculated. For the derivation of these tensors, see Holzapfel (2000).

4. Numerical analysis

We examine the effect of smooth muscle stretch and intracellular calcium ion concentration on active stress generation under physiological boundary conditions using the finite element analysis. Numerical analysis is conducted using an in-house research code developed for analyzing geometric and material nonlinear problems. In the analysis, the arterial segment is considered as a slightly compressible thick-walled cylindrical tube, which is a simplified shape of an artery.

[DOI: 10.1299/jbse.2014jbse0002]

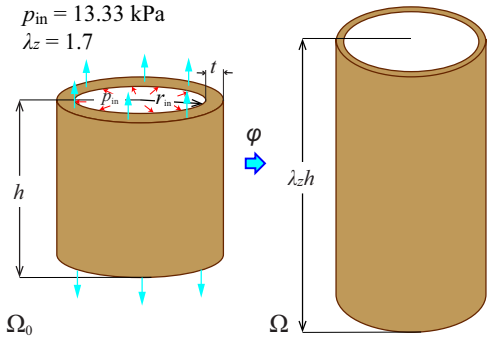

Fig. 3 Schematic of boundary conditions, initial shape, and deformed shape of arterial segment. The thick-walled cylindrical tube is assumed to have a height h of 1.85 mm with an inner radius r_{in} of 3.70 mm and a wall thickness t of 0.77 mm as taken from the swine carotid artery (Stylianopoulos and Barocas, 2007). As boundary conditions, the axial stretch λ_z is set to the approximate axial in situ stretch of a carotid artery (1.7) (Holzapfel et al., 2004), and the inner pressure p_{in} is set to normal blood pressure (13.33 kPa).

4.1. Conditions for the numerical analysis

The initial geometry and applied boundary conditions of the arterial segment are shown in **Fig.** 3. The passive, active, and chemical material parameters of the model are listed in **Tables** 1, 2, and 3. Parameter values are taken from previous works fitted to swine carotid artery.

Because the inner and outer layers are mechanically insignificant, only the middle layer is considered, i.e., the model is single-layered. The body forces are negligible in comparison with the surface traction loads and internal forces. To focus on the relationship between active and passive stresses, we do not consider the effect of residual stresses. The deformation is assumed to progress very slowly, while chemical equilibrium is maintained. We assume that in the reference (initial) configuration, the initial intracellular calcium ion concentration $\beta_0(\boldsymbol{X})$ is uniform throughout the arterial wall ($\beta_0(\boldsymbol{X}) = \beta_0$) and remains constant throughout the arterial deformation, i.e., $\beta_0(\boldsymbol{x}) = \beta_0$. This assumption means that the calcium ion concentration inside and outside the cell has reached equilibrium.

Table 1 Passive and active material parameters in Eqs. (5), (6), (9), and (10).

Parameter	Value	Unit
η	38.4	deg
c_e	3.500	kPa
c_1	23.70	kPa
c_2	1.700	-
γ	4.5	deg
a_0	−4.9	kPa
a_1	−188.2	kPa
a_2	344.5	kPa
a_3	−415.9	kPa
a_4	389.3	kPa
a_5	−124.8	kPa

(Schmitz and Böl, 2011)

Table 2 Chemical parameters in evolution Eq. (7).

Parameter	Value	Unit
k_1	calculated	1/s
k_2	0.50	1/s
k_3	0.40	1/s
k_4	0.10	1/s
k_5	0.010	1/s

(Hai and Murphy, 1988)

Table 3 Chemical parameters in enzyme reaction Eq. (12).

Parameter	Value	Unit
a	−0.0400	-
b	0.686	-
c	0.015	-
d	3.02	-

(Murtada et al., 2010b)

Finite element analysis is conducted under the following conditions: (i) The arterial segment is discretized into 9 radial elements, 160 elements around its circumference, and 9 axial elements, and it is modeled by the hexahedral Q_1/P_0-element (i.e., trilinear displacement and constant Lagrange multiplier approximations). (ii) 10 equal-load increments are applied to the arterial segment. (iii) Newton-Raphson iterations continue until all normalized square residual norms are below 10^{-5}. (iv) The penalty parameter κ is taken to be $c_e \times 10^4$. We use the direct sparse solver PARDISO included in the Intel Math Kernel Library for solving large sparse linear systems and LAPACK routines for eigenvalue and least squares problems.

4.2. Results: Chemical state and Cauchy stress distributions

From the Eqs. (8), (11), and (12), the chemical states α_i as a function of the intracellular calcium ion concentration β_0 at a steady state are plotted in **Fig.** 4. If β_0 is less than 124 nM, then smooth muscle cells are fully relaxed ($\alpha_3 + \alpha_4 = 0$).

[DOI: 10.1299/jbse.2014jbse0002]

If β_0 is greater than approximately 250 nM, then the activation of smooth muscle cells is saturated, as indicated by the red line in **Fig.** 4.

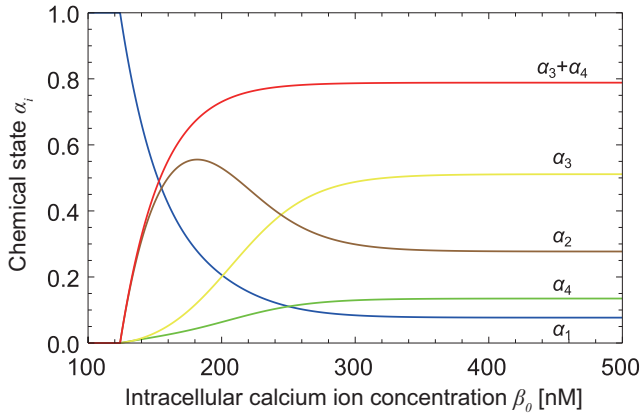

Fig. 4 Relationship between chemical state fractions $\alpha_1, \cdots, \alpha_4$ and the intracellular calcium ion concentration β_0 at the chemically steady state.

The distributions of the Cauchy stress components $\sigma^{\theta\theta}$ and σ^{zz} through the deformed wall thickness as functions of the radial coordinate r, are plotted for various initial calcium ion concentrations β_0 in **Fig.** 5. Because active stresses are generated toward the circumferential and axial directions, we focus on these two stress components. When β_0 is less than 124 nM, active stresses are absent in the arterial wall, indicating a passive response to the external loads. As the intracellular calcium ion concentration β_0 increases, the effect of active stress appears gradually and continuously. In fully activated smooth muscles ($\beta_0 \geq 250$ nM), unlike the case for lower-activated muscles, the principal stress distribution behaves like an almost linear function of r. The stress distribution obtained in the conventional passive only response model corresponds to the case in which β_0 is below 124 nM. The result by Schmitz and Böl (2011), which includes active stress generation, corresponds to the case in which β_0 is more than 250 nM. Interestingly, in our study, as the activation of smooth muscle cells increases, the Cauchy stress at the outer wall exceeds that at the inner wall.

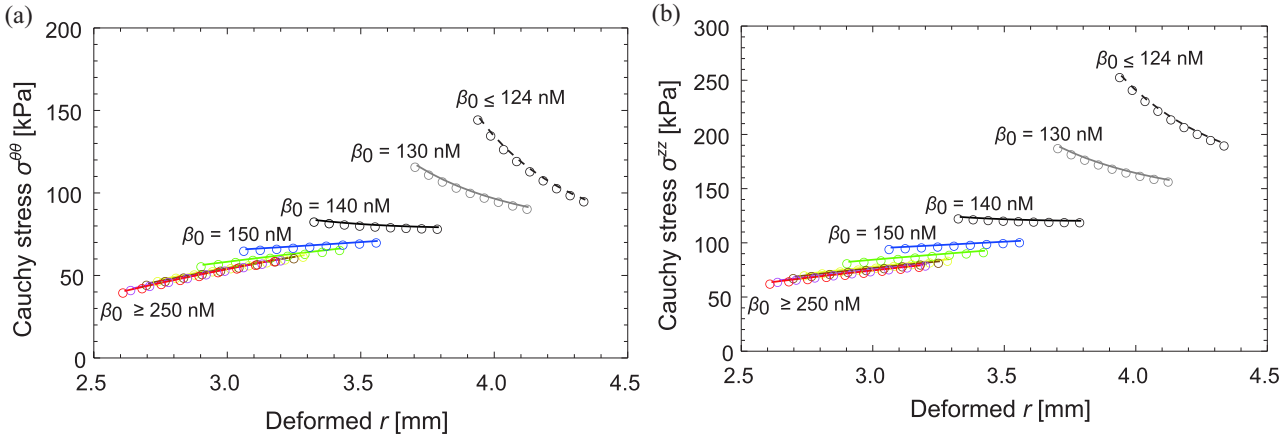

Fig. 5 Elastostatic computation of transmural Cauchy stress distributions at axial stretch of 1.7, inner pressure of 13.33 kPa, and various initial calcium ion concentrations β_0. (a): Circumferential direction. (b): Axial direction.

5. Discussion

In previous literature, active stresses were modeled phenomenologically in the form of a Cauchy stress tensor as a function of smooth muscle stretch, and then, by its integration, strain-energy functions were obtained (Rachev and Hayashi, 1999; Zulliger et al., 2004; Stålhand et al., 2008, 2011; Murtada et al., 2010a,b; Schmitz and Böl, 2011; Böl et al., 2012). By using the finite element method, the mechanical behavior of an arterial wall as described by the strain-energy function including active stresses has been analyzed. From the microscopic viewpoint, active stresses are believed to be generated by the relative sliding between actin and myosin filaments in smooth muscle cells, and they are driven

[DOI: 10.1299/jbse.2014jbse0002]

by chemical reactions (Hai and Murphy, 1988). The probability of active stress generating states has been described in the chemical model regulated by intracellular calcium ion concentration. Although active stress generation is regulated by both smooth muscle stretch and intracellular calcium ion concentration, these two models of active stresses have been studied individually.

In this study, for a better understanding of arterial functions, we developed a mechanochemical model with an active stress generator that couples the chemical model proposed by Hai and Murphy (1988) to the phenomenological mechanical model proposed by Schmitz and Böl (2011). The stress distributions in an arterial wall at each prescribed intracellular calcium ion concentration were calculated by the mechanochemical model using finite element analysis. The differences between the conventional model and our model was that in our model, a spectrum of the stress distributions with respect to various intracellular concentrations concerning the active stress generation can be obtained. Our results were consistent with the fact that active stresses play a role in reducing the stress gradient with respect to radial position r under physiological conditions, and make the stress distribution uniform within the wall beyond the reduction due to residual stress (Yamada et al., 1999, 1997; Humphrey and Na, 2002; Stålhand et al., 2011). Our results also showed that as the intracellular calcium ion concentration β_0 increases, the effect of active stress appears continuously, i.e., stress distribution could be considered as a continuous function of the intracellular calcium ion concentration, and the Cauchy stress at the outer wall exceeded that at the inner wall as the activation of smooth muscle cells increases. This second phenomenon can be explained as follows: (1) In the deformed state, the smooth muscle stretch λ_{m} of the outer portion of the wall is slightly larger than that of inner ones; (2) when the absolute difference between the current stretch λ_{m} and its initial value 1 becomes larger, the smooth muscle cells generate larger active stresses; (3) the behavior of active stress generation changes significantly, when the stretch changes slightly.

The obtained stress distributions could be helpful for understanding the active calcium ion transport systems, because the alterations of the stress distributions caused by the variation of external loads are buffered by proper active stress generation resulting from continuous intracellular calcium ion concentration changes through the active calcium ion transport systems, such as calcium ion channels and ion pumps. In vivo, in order to exert the physiological function of arteries in response to external loads, the adjustment of the intracellular calcium ion concentration by the active calcium ion transport systems will control the stress distribution such that the distribution becomes nearly uniform within the arterial wall, under various physiological state.

Several simplifying assumptions have been made in this study. First, although the intracellular calcium ion concentration varies continuously owing to inflow and outflow from the cell and its storage sites to ensure proper arterial constriction or dilation, calcium ion movements were not considered; to evaluate active stress generation in vivo, active calcium ion transport must be incorporated in the analysis (Yang et al., 2003). Second, this study was conducted under physiological boundary conditions; to evaluate pathogenesis, pathological boundary conditions such as hypertension must be considered. Third, because there are in vivo blood flows inside the cavity of the vessel, fluid-solid interactions cannot be ignored in a computational mechanical approach (Humphrey and Na, 2002).

In a future study, we plan to develop a model that takes into account the active calcium ion transport systems, for example, how stretching of the smooth muscle cells affects the intake of calcium ions from the surroundings. If computational arterial models based on appropriate constitutive laws and boundary conditions are established, physiological functions could be predicted more realistically, leading to improved diagnosis or disease treatment.

Acknowledgements

This research work is supported partly by the Funding Program for Next Generation World-Leading Researchers (LR017) from the Ministry of Education, Culture, Sports, Science and Technology (MEXT) in Japan.

References

Böl M., Schmitz A., Nowak G. and Siebert T., A three-dimensional chemo-mechanical continuum model for smooth muscle contraction, Journal of the mechanical behavior of biomedical materials, Vol.13, (2012), pp.215-229.

Brink U. and Stein E., On some mixed finite element methods for incompressible and nearly incompressible finite elasticity, Computational Mechanics, Vol.19, (1996), pp.105-119.

Chang T. Y. P., Saleeb A. F. and Li G., Large strain analysis of rubber-like materials based on a perturbed Lagrangian variational principle, Computational Mechanics, Vol.8, (1991), pp.221-233.

[DOI: 10.1299/jbse.2014jbse0002]

Fung Y. C., Fronek K. and Patitucci P., Pseudoelasticity of arteries and of its mathematical expression, American Journal of Physiology, Vol.237 (1979), pp.H620-H631.

Gasser T. C., Ogden R. W. and Holzapfel G. A., Hyperelastic modelling of arterial layers with distributed collagen fibre orientations, Journal of Royal Society Interface, Vol.3 (2006), pp.15-35.

Hai C. M. and Murphy R. A., Cross-bridge phosphorylation and regulation of latch state in smooth muscle, American Journal of Physiology - Cell Physiology, Vol.254 (1988), pp.C99-C106.

Holzapfel G. A., Nonlinear solid mechanics: A continuum approach for engineering. John Wiley & Sons, LTD. (2000).

Holzapfel G. A. and Gasser T. C., A new constitutive framework for arterial wall mechanics and a comparative study of material models, Journal of Elasticity, Vol.61 (2000), pp.1-48.

Holzapfel G. A., Gasser T. C. and Ogden R. W., Comparison of a multi-layer structural model for arterial walls with a fung-type model, and issues of material stability, Journal of Biomechanical Engineering, Vol.126 (2004), pp.264-275.

Humphrey J. D. and Na S., Elastodynamics and arterial wall stress, Annals of Biomedical Engineering, Vol.30 (2002), pp.509-523.

Murtada S. I., Kroon M. and Holzapfel G. A., A calcium-driven mechanochemical model for prediction of force generation in smooth muscle, Biomechanics and modeling in mechanobiology, Vol.9 (2010a), pp.749-762.

Murtada S. I., Kroon M. and Holzapfel G. A., Modeling the dispersion effects of contractile fibers in smooth muscles, Journal of the Mechanics and Physics of Solids, Vol.58 (2010b), pp.2065-2082.

Rachev A. and Hayashi K., Theoretical study of the effects of vascular smooth muscle contraction on strain and stress distributions in arteries, Annals of Biomedical Engineering, Vol.27 (1999), pp.459-468.

Rüter M. and Stein E., Analysis, finite element computation and error estimation in transversely isotropic nearly incompressible finite elasticity, Computer methods in applied mechanics and engineering, Vol.190 (2000), pp.519-541.

Schmitz A. and Böl M., On a phenomenological model for active smooth muscle contraction, Journal of biomechanics, Vol.44 (2011), pp.2090-2095.

Stålhand J., Klarbring A. and Holzapfel G. A., Smooth muscle contraction: Mechanochemical formulation for homogeneous finite strains, Progress in biophysics and molecular biology, Vol.96 (2008), pp.465-481.

Stålhand J., Klarbring A. and Holzapfel G. A., A mechanochemical 3D continuum model for smooth muscle contraction under finite strains, Journal of theoretical biology, Vol.268 (2011), pp.120-130.

Stylianopoulos T. and Barocas V. H., Multiscale, structure-based modeling for the elastic mechanical behavior of arterial walls, Journal of Biomechanical Engineering, Vol.129 (2007), pp.611-618.

Sussman T. and Bathe K. J., A finite element formulation for nonlinear incompressible elastic and inelastic analysis, Computers & Structures, Vol.26 (1987), pp.357-409.

Weiss J. A., Maker B. N. and Govindjee S., Finite element implementation of incompressible, transversely isotropic hyperelasticity, Computer methods in applied mechanics and engineering, Vol.135 (1996), pp.107-128.

Yamada H., Shinoda T., Tanaka E. and Yamamoto S., Finite element modeling and numerical simulation of the artery in active state, JSME Int. J. Series C, Mechanical systems, machine elements and manufacturing, Vol.42 (1999), pp.501-507.

Yamada H., A mathematical model of arteries in the active state (incorporation of active stress and activation parameter), Trans. The Japan Society of Mechanical Engineers (in Japanese), Vol.63 (1997), pp.2257-2262.

Yang J., Clark J. W., Bryan R. M. and Robertson C. S., The myogenic response in isolated rat cerebrovascular arteries: Vessel model, Medical Engineering & Physics, Vol.25 (2003), pp.711-717.

Zulliger M. A., Rachev A. and Stergiopulos N., A constitutive formulation of arterial mechanics including vascular smooth muscle tone, American journal of physiology Heart and circulatory physiology, Vol.287 (2004), pp.H1335-H1343.

[DOI: 10.1299/jbse.2014jbse0002]